Egyptian Geophysical Society
EGS Journal, vol. 5, No. 1, 25-32 (2007)

DETERMINING CAUSES OF STRUCTURAL BUILDING DAMAGES IN 15TH OF MAY CITY, CAIRO, EGYPT, USING GEOPHYSICAL AND GEOTECHNICAL APPLICATIONS

T. Abdel-Hafez

National Research Institute of Astronomy and Geophysics, 11722 Helwan, Cairo, Egypt.

تحديد أسباب الإنـهيارات فى المبانى بمدينـة ١٥ مايو بإستخدام التطبيقات الجيوفيزيقية والجيوتقنية ، القاهرة – مصر

الخلاصــة: مدينـة ١٥ مـايو من المنـاطق العمرانيـة الجديدة التى تم إنشاؤها منذ حوالى ٢٥ عاماً تقريباً. حيث تم بناؤها على صـخور الحجر الجيرى التى تنتمى إلى العصر الإيوسيني. وبالرغم من أنه لم يمرعلى بنائها وقت طويل إلا أن مبانيها تعرضت إلى بعض التصدعات والشروخ الخطيرة منذ ما يقرب من ١٠ سنوات. وبما أن الأسباب وراء هذه التصدعات غير معلومة، فقد تمت هذه الدراسة بإستخدام التطبيقات الجيوفيزيقية والجيوتقنية وذلك لتحديد اسباب هذه التصدعات. ولقد تم عمل ٤ بروفيلات جيوكهربية بإستخدام أشكال ديبول– ديبول حيث أظهرت نتائج الدراسة عن وجود مناطق تحتسطحية ذات مقاومات نوعية مختلفة. وتظهر المناطق الجيوكهربية ذات المقاومة النوعية الأدنى عن وجود الرسوبيات الطفلية المتداخلة مع رسوبيات الحجر الجيرى ، بينما تظهر المناطق الجيوكهربية ذات المقاومة النوعية العالية عن وجود رسوبيات الحجر الجيرى. كما أظهر المسح الإلكترونى لعينات الصـخور الطفلية وجود بعض الفراغات والشروخ الدقيقة وشريط رقيق من الرسوبيات الملحية التى تغطى المعادن الطفلية والجيرية. ونتيجة لتفاعل المعادن الطفلية والملح مع المياه الجوفية المتسربة التى ظهرت أخيراً بمدينـة ١٥ مـايو أدى ذلك إلى التصدعات والشروخ الخطيرة فـى مبـان المدينـة. ونوصـى بقوة أن تؤخذ فـى الإعتبـار إستخدام التطبيقات الجيوفيزيقية والجيوتقنية قبل البدء فى إنشاء المناطق العمرانية مستقبلاً.

ABSTRACT: *The 15th of May City is a suburb in the south of Cairo that developed over the last 25 years. The city is built on Eocene sedimentary rocks of mainly limestone. Despite its young age, the city has many buildings with severe structural damage, which mainly developed over the last 10 years. The reasons for the structural damage were unknown and led to this study. Both geophysical and geotechnical investigations were carried out in order to determine these causes. Four geoelectric profiles with dipole-dipole arrays have been carried out. The results of these geoelectric investigations identified the existence of different geoelectric zones with different resistivities in the subsurface. The lowest resistivity in the geoelectric zone reveals shale deposits intercalated with limestone rocks while the high resistivity reveals only limestone bedrock. Scanning electron microscopy (SEM) analysis of the Eocene shale shows pores and micro-cracks with thin films of salts, mainly halite, covering the carbonate and clay minerals. As a result, the interaction of clay minerals and salts with groundwater seepage, most likely is the geo-technical problem causing the cracking of the buildings in the 15th of May City. It is strongly recommend that geophysical and geotechnical investigations should be taken into account before any further constructions at the new suburbs.*

INTRODUCTION

The River Nile in Egypt flows from south to north and is considered to be the life vein for Egyptians over the last 3500 years, mainly due to its highly productive floodplains on both sides of the river. Bordering the fertile river floodplains are the eastern and western desert with limestone bedrock exposed in the northern Nile Valley. Due to insufficient accommodation space for an increasing population, the Egyptian government enlarged this urban area by building new developments on its periphery, to both the east and west of the Nile Valley.

The 15th of May City (Figure1) is new urban development, which lies about 140 m above the River Nile and is built on Eocene strata. The Eocene sediments consist of mainly intercalated beds of marine limestone and thin beds of shale. In most outcrops, fissures and cracks of the limestone bedrock are covered with halite crystals. It is well known that these Eocene limestones are karstified and contain caves. The development of the 15th of May City showed that after inhabitation, water infiltrated beneath some of the buildings. The reasons for the water infiltration underneath newly constructed or under construction remaining houses were unclear but it was observed during this study that drainage pipe repairs significantly reduced the water level underneath some houses. The level of this infiltrated water was not determined but fluctuated markedly according to observations of inhabitants and this study. However, after such water level changes, damages to the building started to develop including wall and ceiling cracks. This was also observed in a primary school. The government assigned two scientific groups to study the deterioration of the buildings and some buildings were evacuated. Occupants have since returned to their buildings and the government is now constructing further buildings. Similar marked deteriorations of buildings were also observed and described from the main rest house in the Valley of the Kings, Luxor, Egypt, that was built in 1990 and drainage water affected the underlying Eocene shale units that led to ground heave and hence lifting of selected parts of the building (Wüst 2000a).

Elawadi, et al. (2006), concluded in his geophysical study that, the dominant features in the interpreted geophysical sections are vertical to nearly-vertical fractured zones, contacts, and joints detected by GPR. These features, common in this type of limestone, could be seen in a limestone quarry near to the investigated site. These fractures associated with karstic features are considered to be the main hazard of the construction of the buildings in the study area. Also, he concluded that this hazard has been increased by two factors. The first is uncontrolled use of the surface water for irrigation in the main garden as well as gardens between the buildings that activate the dissolution process and facilitate the movements along the fracture planes. The second is the use of dynamite in the limestone quarry very near to the town.

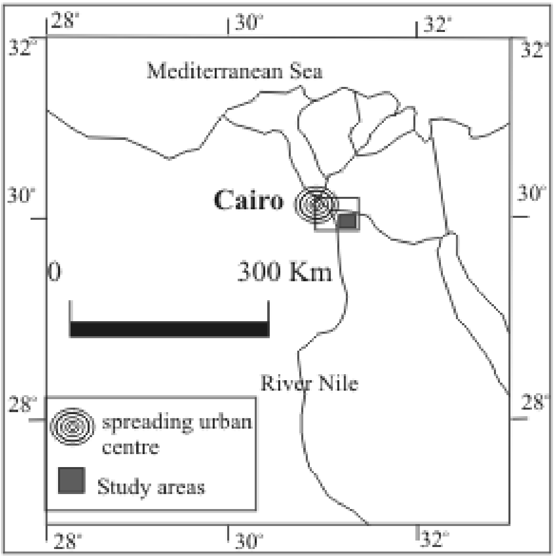

Figure 1. Location map of the study area in the 15th of May City, SE of Cairo.

Figure 2. Documentation of building damage features in District No.17, 15th of May City. Photos were taken on 15/6/2005.

The aim of this study is to examine possible causes of building damages observed in the 15th of May city (Figure 2), particularly in District No.17 (a small territory in the City). The methods used are two dimensional geoelectric imaging and other geotechnical techniques. The purpose of using geoelectric imaging is to identify the shale intercalations and defining possibly cavities or karstic features, while the geotechnical investigation were done to determine the properties of the rocks.

Geological Settings

The 15th of May City is located east of the Nile Valley and south of Cairo (Figure 1). To the east and the west of the Nile Valley, the desert begins as soon as the floodplain ends which is marked by terraces that are relicts of the time when the River Nile eroded through the Eocene/Oligocene bedrock during the Miocene (Said, 1990). These terraces are the type section of Observatory subgroup of Eocene rocks which are located at Observatory Plateau at Helwan City. The Observatory subgroup is divided into Gebel Hof and Observatory Formations by Farag and Ismail (1959).

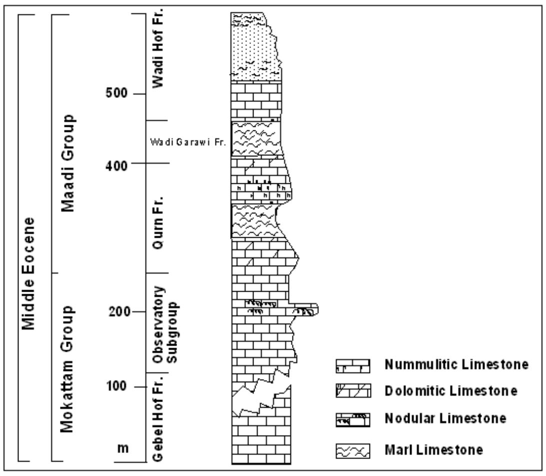

Figure 3. Stratigraphic section of the study area (after Strugo, 1986).

The Gebel Hof Formation is 121 m thick (base unexposed) (Figure 3) and is made up of a 100 m thick fine-grained, non fossiliferous limestone, becoming nummulitic toward the top. This formation is followed by a 21 m thick, extensively burrowed limestone unit containing *Nummulities gizehensis*. These nummulite species indicates Middle Eocene age. The Observatory Formation is overlying the Gebel Hof Formation which is made up of 136 m of limestones and chalky limestones of varying textures. The beds of this unit may be burrowed, laminated, thin-bedded, nodular, soft, hard or dolomized limestone.

Field Observation

Some veins of halite crystals, some of which several centimeters thick, and thin beds of shale occurred in the study area wherever the bedrock outcrops in the study area of District No.17 (Figure 4c). There, also layers or lenses of gypsum were observed with some of the gypsum filling cracks and fissures of the limestone bedrock. At the same time, cavities and caves were also observed in the study area and around Gebel Hof (Figure 4d). Figure 4a illustrates that some of the buildings were constructed along the cliffs of the Formation that is composed of shale/limestone interbeds that also contained gypsum lenses.

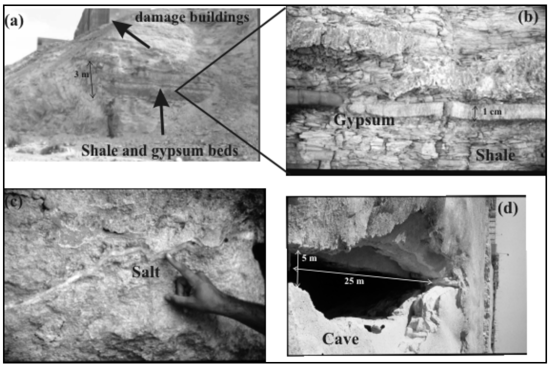

Figure 4: Bedrock illustration from the field area including; a) cliff/terrace outcrop showing shale/limestone interbeds of the Observatory subgroup and buildings constructed above, b) Gypsum lens interbedded in the shale/ limestone bedrock (see Fig. 4a for location), c) Salt vein in limestone bedrock, and d) open cave along the cliffs/terraces,

METHODOLOGY

Geoelectric resistivity imaging introduces an electric current into the ground with two electrodes and voltage (current flow) changes are recorded by two other electrodes. In order to conduct the geoelectric survey, SYSCAL R2 of IRIS instruments is used, which is controlled fully by a computer via serial link. The injection current rage of the instrument is from 0.5A to 2A while the voltage ranges from 100V to 800V. The voltage supply for injection current is from the mains via the usual AC/DC converter. Measurements are carried out using many cycles of direct current with alternating sign and 6 stacking.

A multi-electrode switch box was built with special relays. It can accommodate up to 480 electrodes; it is also able to check electrode configurations for their correctness so short circuits and zero connections are avoided. The electrodes are made up of common steel with length of 50 cm and a diameter of 2 cm. They are inserted into ground. Because the rock is usually dry and the contact resistances are very high, the electrodes had to be moistened occasionally. The electrodes are installed along profiles with 5 m electrode spacing. For the measurements the usual four point configuration is used with two electrodes for the injection of the current and another two electrodes to measure the field.

A dipole-Dipole array is used (Kurz, 1997) in this survey because it has low EM coupling between the current and potential circuits (Loke, 1998). Also, this array is sensitive to horizontal changes in resistivity. The inversion of the apparent resistivities are calculated using the program RES2DINV (Barker, 1992; Loke, 1995) which is based on a least square iterative algorithm. The measurements provide information on the electrical behavior of the material below the surface. The distance between the electrodes determines the depth of investigations. Geoelectric resistivity imaging profiles are produced by modeling the data from a series of measurements with different depths and locations along a survey line (Baines 2002). Four geoelectric profiles were collected using dipole-dipole array with 5 m electrode spacing and 32-48 electrodes (Figure 5).

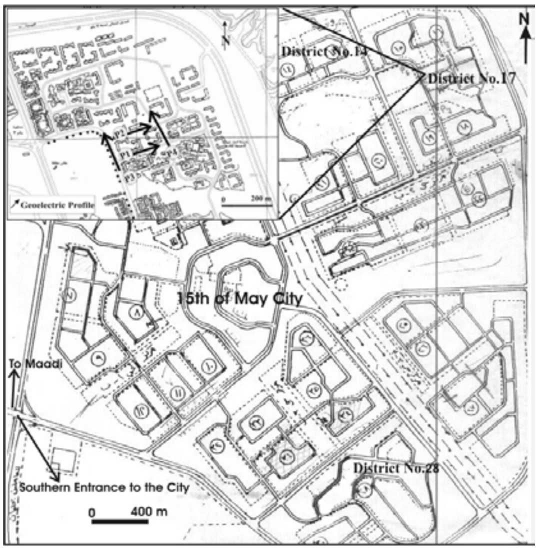

Figure 5. Map of District No.17 in the NE part of 15th of May City, showing the location of the four geoelectric profiles.

The sedimentological and mineralogical composition of the bedrock defines the properties of the rock itself, and determined the geotechnical behavior of the material. A Scanning Electron Microscopy (SEM**)** imaging system coupled with an Energy Dispersive System (EDS) (***CamScan CS4)*** was used to characterize rock surfaces and the mineral composition. The rock samples were collected from the shale and gypsum outcrops located in the 15th of May City (see Figure 4a and b). These outcrops are part of the Observatory subgroup composed of limestone with shale interbeds

RESULTS

Geophysical analysis

Geoelectric profile P1 measured with electrode spacing of 5 m (Figure 6) shows existence of two geoelectric zones.

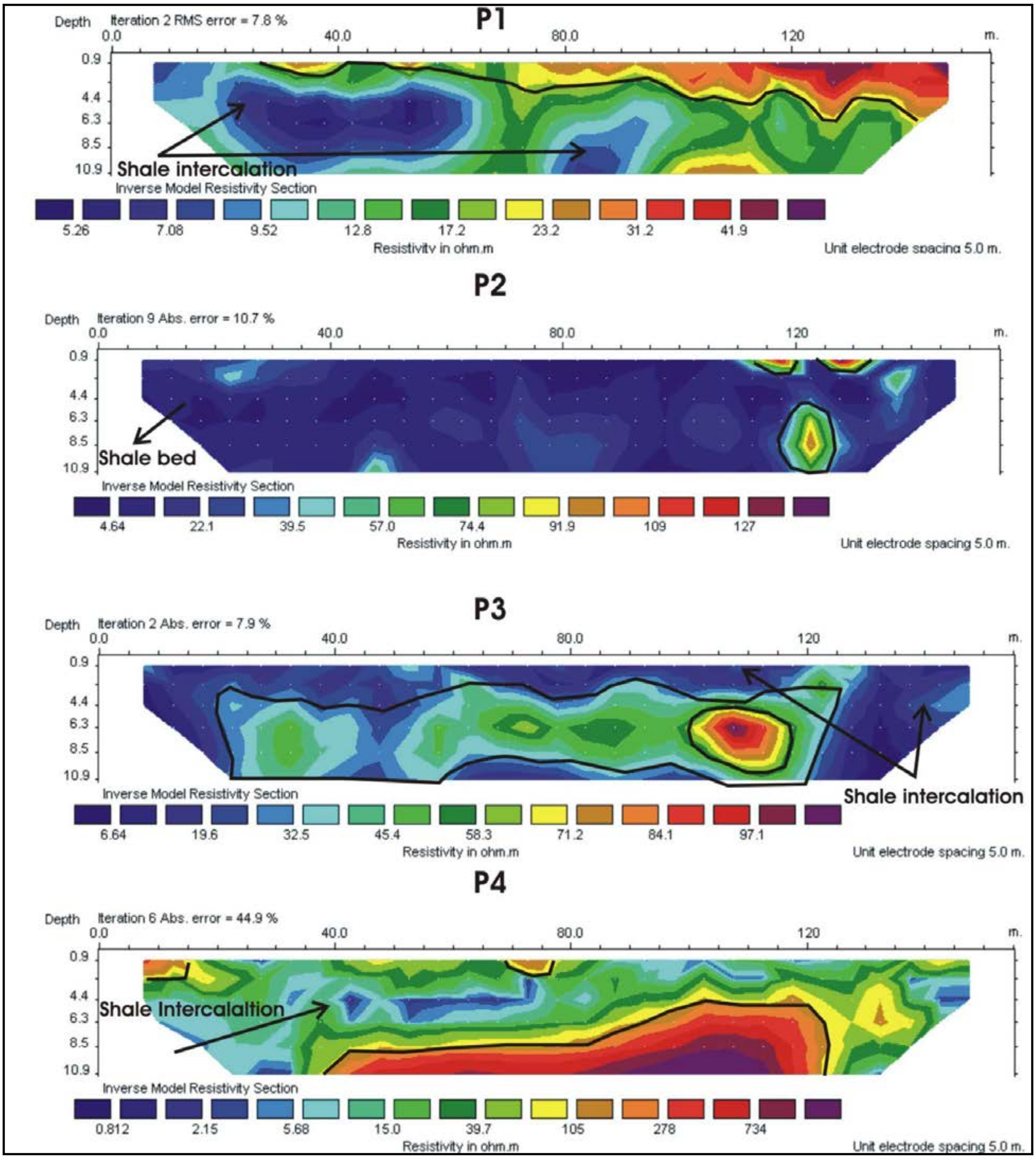

Figure 6. Geoelectric Profiles (for location see Figure 5).

The first 30 m are characterized by a low resistivity zone after which the resistivity changes markedly. There, the resistivity ranges from 23 to 50 Ohm.m and extends all the way to the end of the profile. The geoelectric zone detected at the beginning of the profile dips into the subsurface after 30 m with a shallow angle. The resistivity of this zone ranges between 5-13 Ohm.m. The thickness of this zone ranges from >11 m at the beginning of the profile to approximately 4 m at the end of the profile, where a high (~23 Ohm.m) resistivity layer occurs underneath it.

Geoelectric profile P2 measured with electrode spacing of 5 m (Figure 6) shows existence of one low resistivity zone with intercalation of high resistivity zone. This high zone has resistivity > 127 Ohm.m and is marked at 120 m on the top of the profile and on 6 m depth. . The low resistivity zone is marked at the beginning of the profile with < 10 Ohm.m and extends all the way to the end of the profile. The thickness of this zone geoelectric zone is approximately 10 m.

Geoelectric profile P3 (Figure 6) measured with an electrode spacing of 5 m, also shows existence of two geoelectric zones. The first zone is characterized by low resistivity < 10 Ohm.m at the beginning of the profile and extends all the way to the end of the profile. The thickness of this zone ranges from 5 m at the beginning of the profile to approximately 11 m at the end of the profile. The second zone has relatively high resistivity ranges from 32-97 Ohm.m with thickness 6 m approximately. This second zone is marked at between 20-120 m. This zone has high resistivity spot at 100 m from the beginning of the profile and on 5 m depth approximately.

Geoelectric profile P4 measured with an electrode spacing of 5 m (Figure 6) shows existence of two geoelectric zones. The resistivity of the first zone is < 15 Ohm.m with 11 m thickness at the beginning of the profile. This thickness decreases to 5 m between the surface distance of 100-120 m. The second zone has high resistivity > 700 Ohm.m and is marked on 8 m depth between the surface distances of 40-120 m.

Mineralogical analysis

SEM photomicrographs of shale samples from the Observatory subgroup along and vertical to the bedding planes were collected to identify mineralogical and sedimentological features (Figure 7). Micro- and microspores were observed (Figure 7a, b) with halite crystals in the matrix (Figure 7b). The matrix contains abundant halite minerals that cover the carbonate and clay minerals (Figure 7c) forming a thin film in some instances (Figure 7c). In addition, gypsum crystals could be identified in the SEM photomicrographs (Figure 7d).

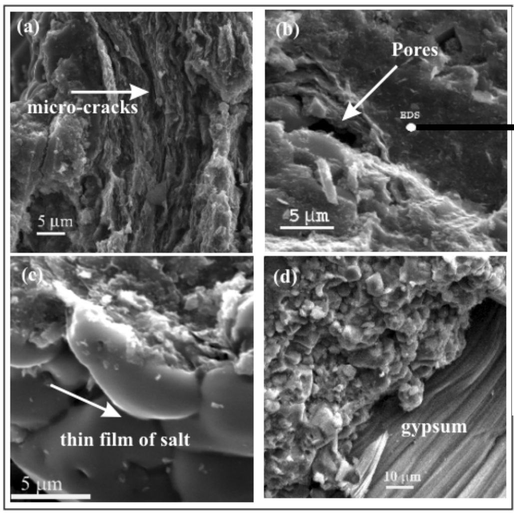

SEM photomicrograph of some aspects of Eocene Shale: a vertical to the bedding plane; b & c along the bedding plane and d for gypsum rock sample

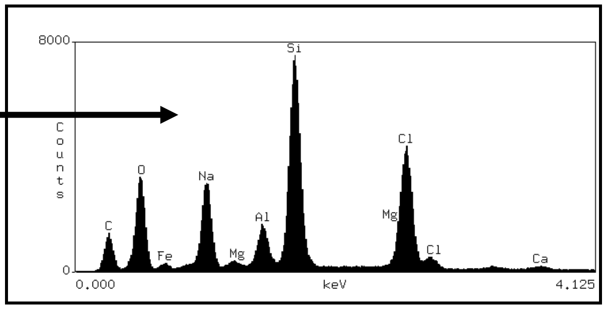

EDS analysis result of specific area as shown by arrow

Figure 7. SEM photomicrographs and EDS analysis of shale samples from District No.17, 15th of May City.

DISCUSSION

Many geophysical methods are suitable for imaging the subsurface with limitations. Electromagnetic waves (EM) are attenuated strongly in moist areas, i.e., the depth of investigation is rather limited. Further limitation is due to strong reflections from geological features such as thin moist clay layers, and the transmission beyond these layers is not possible (Yaramanci, 2000). Because the moist areas are not penetrated by EM, geoelectric investigation is utilized and adopted. A dipole-Dipole array is used in this survey because it has low EM coupling between the current and potential circuits (Loke, 1998). Also, this array is sensitive to horizontal changes in sistivity. In addition, this method is quick, inexpensive and uses non-invasive means to provide information about the subsurface properties, depth to bedrock, location and distribution of conductive fluids (Reynolds, 1997).

The geoelectrical data collected by dipole-dipole array were processed and interpreted to image the subsurface beds at the investigated site. The study shows the existence of two different resistivity zones with different thicknesses (Figure 6).

The high resistivity zone delineated in the geoelectric profiles P1 has average resistivity range about 100 Ohm.m (Figure 6) is interpreted as limestone partially saturated with water seepage (Van Nostrand, 1966, Elawadi et al. 2006). The high resistivity spots detected in Profile P2 at 120 m on the surface and 4 m depth are interpreted as partially saturated limestone boulders or blocks which have been confirmed by digging at the location of shallower one (Elawadi et al., 2006). The high resistivity spot (> 90 Ohm.m) detected in the geoelectric profile P3 on 6 m depth at the surface distance100 m (Figure 6) is interpreted as partially saturated hard limestone block. The high resistivity spots (> 100 Ohm.m) detected in Profile P4 (Figure 6) on the top of the profile at the surface distances 10 m and 75 m are interpreted as partially saturated hard limestone blocks; while the high resistivity zone (> 700 Ohm.m) detected at the surface distances between 40-120 m on a depth of about 8 m is interpreted as dry hard limestone bedrock.

In Figure 6, all geolectric profiles show that the average of low resistivity anomalies zones (~10 Ohm.m). These zones are interpreted as pocket of shale saturated with water. The high resistivity zones detected in the profiles were interpreted as hard limestone blocks which has been confirmed by Elawadi (2006).

In the limestone bedrock of the study area, infiltrated water dissolves halite first, then anhydrite. In addition to those minerals, the shale beds in this limestone bedrock of Observatory subgroup has high content of swelling clay minerals (smectite), which accelerate the deterioration of District No.17 due to swelling and shrinkage effects.(Abdel-Hafez 2004).

Halite crystals are observed in the SEM photomicrographs (Figure 7b). Most salts, including chlorides have high coefficients of volumetric expansion and show a volume increase with higher temperature (Cooke and Smalley, 1968). Halite in solution is mobile and can result in substantial pressure build up that leads to rupture. During drying, halite grows by adsorbing sodium and chloride ions from surrounding connected pores; then, evaporation of the water enables halite crystals to grow and exert pressure on the overlying beds, which cause cracks developments (Wüst 2000a).

Micro-crackes and pores in the rock's internal structure of the collected rock sample (Figure 7a and 7b) are observed, which could produce deterioration to the adjacent beds when they are uploaded. Gypsum crystals are also observed (Figure 7c) in the geotechnical analysis. The EDS analysis (Figure 7) show that the rock samples contain clay minerals such as smectite. Wüst (2000a), described that the deterioration in the Royal tomb of Seti I, is due to shrinkage and swelling process of smecitite clay minerals, and due to volume changes of anhydrite. During, hydration, anhydrite changes to gypsum and may expand its volume (Wittke et al., 1984).

CONCLUSION

In the present study, an integrated geophysical and geotechnical applications were carried out in District No.17 at 15th of May City, south Cairo, Egypt. Despite its young age, the city has many buildings with severe structural damage. The objectives of these investigations were to image the subsurface of the affected area to determine the causes behind these structural damages. 2D resistivity profiling using dipole-dipole array with 5 m electrode spacing and geotechnical analysis were applied. The geoelectric data collected were processed and interpreted to delineate the existence of shale beds. Two resistivity zones were distinguished in the geoelectric profiles. Based on the geophysical signature of these zones, the low resistivity zones in all geolectric profiles were interpreted as shale pockets saturated with water. The high resistivity spots in profiles 2 and 3 were interpreted as limestone blocks. The high resistivity spots on the surface of the profile 4 were also interpreted as limestone blocks partially saturated with water, while the high resistivity zone (> 700 Ohm.m) in the same profile was interpreted as dry limestone bedrock.

Salts which are mainly halite, pores and micro-cracks in the rock's internal structure can contribute to the structural damage potential at District No.17 in existence/absence of water. Salts interact with water seepage and can be dissolved causing deterioration to the adjacent beds. During drying salts adsorb sodium and chlorides ions of waters from surrounding pores; then evaporation of the water enables halite crystals to grow and increase pressure on the surrounding adjacent beds (Wüst 2000b). Furthermore, structural damage could originate from the expansive clay minerals of the delineated shale. Modern implications can be seen at the new rest house in the Valley of the Kings that was built in 1990. There, the swelling of shale resulted in a 5-7 cm wide crack observed in 1994. The water causing the swelling originated from leaking septic tank underneath the rest house (Wüst 2000b). I have observed during a field trip on 2003 that the rest house is completely collapsed.

As District No.17 and others but not all the city suffer from damages in constructions, and infiltrated water was observed underneath some of the buildings in District No.17, therefore it can be concluded that existence of water was a good environment to shale beds, halite and gypsum to react causing chemical weathering changes that can lead to cracks in the building and damage potential.

Such investigations should contribute to answer the question of the origin of building damages as observed, and also to a question of building in desert is secure or not. The contribution of karstified limestone and mineralogically sensitive clays can be geotechnically problematical. This paper presents first result of ongoing research. A detailed damage mapping for the new urban centre is in preparation.

The author urges the government to take this problem into consideration during the ongoing and further constructions. Also, I recommend further detailed studies to delineate the origin of this water seepage and possible ways to control its quantity and passes.

ACKNOWLEDGEMENT

I would like to express my appreciation to the staff member of the Institute for Geological Sciences, Bern University, Switzerland, for their help in analyzing the collected rock samples. Special thanks to the staff of The Geoelectricity Lab, National Research Institute of Astronomy and Geophysics for their help and encouragements.

REFERENCES

Abdel-Hafez, T., 2004: Geophysical and geotechnical studies in pharaonic and urban Egypt.PhD Thesis, University of Berne, Switzerland. 113 p.

Baines, D., 2002 : Electrical Resistivity ground Imaging (ERGI): a new mapping the lithology and geometry of channel-belts and valley-fills. Sedimentology 49, 441-449

Barker R.D., 1992: A simple algorithm for geoelectrical imaging of the subsurface. First Break 10, 53-62

Barshad. I., 1955: Adsorptive and Swelling Properties of Clay-Water System. First National Conference on Clays and Clays Technology, Dep. of Natural Resources, Division of Mines,San Francisco, Bull. 169, 70-77.

Brattli, B., and Broch, E., 1995: Stability problems in water tunnels caused by expandable minerals. Swelling pressure measurements and mineralogical analysis. Engineering Geolgy 39, 151-169

Cooke, R.U., and Smalley, I.J., 1968: Salt weathering in deserts. Nature, 220, 1226-1227

Elawadi, E., El-Qady, G., Nigm, A., Shaaban, F., and Ushijima, K., 2006: Geophysical survey at a new Dwelling area, Egypt. Journal of Environmental and Engineering Geophysics 11 Issue 4, 249-259

Farag, I.A.M., and Isamil, M.M., 1959: A contribution to the structure of the area east of Helwan, Egypt. J. Geol. 3, 71-86

Griffiths D.H., Turnbull, J., and Olayinka, A.I., 1990: Two dimensional resistivity mapping with a computer controlled array. First Break, 8, 121-129

Kurz, G., 1997: Untersuchung zur geoelecktrischen Uebrwachung des Salinars im Forschungsbergwerk Asse. MSc Thesis, Technical University Berlin

Loke, M.H.D., 1995: Users Manual to RES2DINV, 2D resisitivity inversion using Gauss-Broyden Least-squares method. Campus Geophysical Instrument, England

Loke, M.H.D., 1998: RES2DINV, Rapid 2D resisitivity and IP inversion using least-square methods. User Mannual, Austin Tex., Advanced Geoscience, Inc., 66 p.

Loke, M.H.D., 1999: Res2dinv software User's Manual, Version 3.4. Penang, Malysia, 81 p.

Lutenegger, A.J., Wollenhaupt, N.C., and Handy, R.L., 1979: Laboratory simulation of shale expansion by induced gypsum growth. Canadian Geotechnical Journal, 16, 405-409.

Reynolds, J.M., 1997: An Introduction to Applied and Environmental Geophysics. Wiley, New York, 796 p. Said, R., 1990: The geology of Egypt. A.A. Balkema, Rotterdam, Brookfield, 734 p.

Strougo, A., 1986: Mokattam stratigraphy of eastern Maghagha-El fashn district. Middle East Res. Center, Ain Shams Univ., Sci. Res. Series, 6, 33-58.

Van Nostrand, R.G., and Cook, K.L., 1966: Interpretation of resistivity data. U.S Geol. Survey, Prof. Paper 499

Wittke, W., Semprich, S., and Plischke, B., 1984: Felsmechanik; Grunlagen fuer wirtschaftliches Bauen in Fels. Springer Berlin, 1050

Wüst, R.A.J. and McLane, J., 2000a: Rock deformation in the Royal Tomb of Seti I in the Valley of Kings, Luxor, Egypt. Engineering Geology, 58, 163-190

Wüst, R.A.J., and Schlüchter, C., 2000b: The origin of the soluble salts in Rocks of Thebes Mountains, Egypt: The damage potential to Ancient Egyptian Wall Art. Journal of Archaeological Sciences, 27, 1161-1172

Yaramanci, U., 2000: Geolectric exploration and monitoring in rock salt for safety assessment of underground waste disposals sites. Journal of Applied Geophysics, 44, 181-196